Investigation of MoS_2 and Graphene Nanosheets by Magnetic Force Microscopy

Hai Li,[†] Xiaoying Qi,[‡] Jumiati Wu,[†] Zhiyuan Zeng,[†] Jun Wei,[‡] and Hua Zhang[†,*]

[†]School of Materials Science and Engineering, Nanyang Technological University, 50 Nanyang Avenue, Singapore 639798, Singapore, and [‡]Singapore Institute of Manufacturing Technology, 71 Nanyang Drive, Singapore 638075, Singapore

ABSTRACT For the first time, magnetic force microscopy (MFM) is used to characterize the mechanically exfoliated single- and few-layer MoS_2 and graphene nanosheets. By analysis of the phase and amplitude shifts, the magnetic response of MoS_2 and graphene nanosheets exhibits the dependence on their layer number. However, the solution-processed single-layer MoS_2 nanosheet shows the reverse magnetic signal to the mechanically exfoliated one, and the graphene oxide nanosheet has not shown any detectable magnetic signal. Importantly, graphene and MoS_2 flakes become nonmagnetic when they exceed a certain thickness.

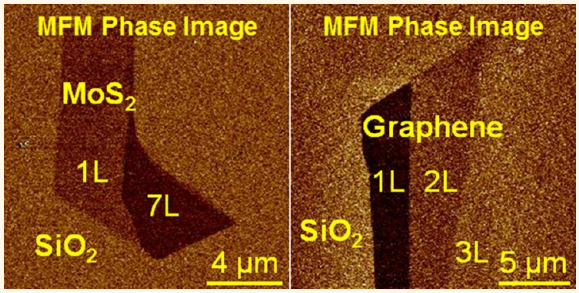

KEYWORDS: magnetic force microscopy · MoS_2 · graphene · nanosheet · phase shift

Owing to their unusual electronic structures and exceptional physical properties, two-dimensional (2D) layered nanomaterials have received numerous attention in recent years.[1−12] Graphene, a single-layer 2D carbon material with zero band gap, is the most studied 2D nanomaterial and shows extensive applications due to its fascinating properties, such as high electron mobility, good thermal conductivity, excellent elasticity, and mechanical stiffness.[4,5,7,9] Recently, the layered transition metal dichalcogenides (TMDs) have also attracted increasing interest due to their unique physical properties, such as the ideal band gap and large in-plane electron mobility.[1−3,5,6,8,13−19] Among them, MoS_2 shows great applications in transistors,[8,17,20] sensors,[3,21,22] memory devices,[23,24] and hydrogen evolution.[25,26]

Compared to the extensive experimental and theoretical studies on electrical, mechanical, and optical properties of atomically thin graphene and MoS_2 nanosheets, only a few studies on their magnetic properties have been reported.[27−34] It is known that the bulk graphite is diamagnetic and single crystal MoS_2 is nonmagnetic.[27,35,36] However, the atomically thin 2D nanosheet usually gives novel physical properties compared to its bulk material due to the quantum and surface effects. Recently, the room-temperature ferromagnetism of reduced graphene oxide (rGO) has been reported through the measurement by magnetometer.[28,29,32] In addition, the room-temperature magnetic properties of multilayered functionalized epitaxial graphene on SiC wafers have also been measured by magnetic force microscopy (MFM) and scanning tunneling microscopy (STM).[37,38] The MoS_2 thin film with typical edge dimension of ~100 nm has exhibited weak magnetism, which is attributed to the existence of the zigzag edges in the ferromagnetic ground state.[27,31] As the thickness and grain size decrease, the increase of magnetism has been observed in both graphene and MoS_2 thin films.[27,28,31] To date, the mechanical exfoliation is still the easiest and fastest way to produce high-quality, atomically thin nanosheets of single-crystal 2D layered nanomaterials, which are suitable for fundamental studies.[2,3,5,8,12,13,16,17,31] Although the theoretical calculation can predict the magnetic property of individual single- or few-layer graphene and MoS_2 nanosheets,[32−34] to the best of our knowledge, there is no direct experimental study of the magnetic response of individual, mechanically

* Address correspondence to hzhang@ntu.edu.sg, hzhang166@yahoo.com.

Received for review January 27, 2013 and accepted February 26, 2013.

Published online February 26, 2013
10.1021/nn400443u

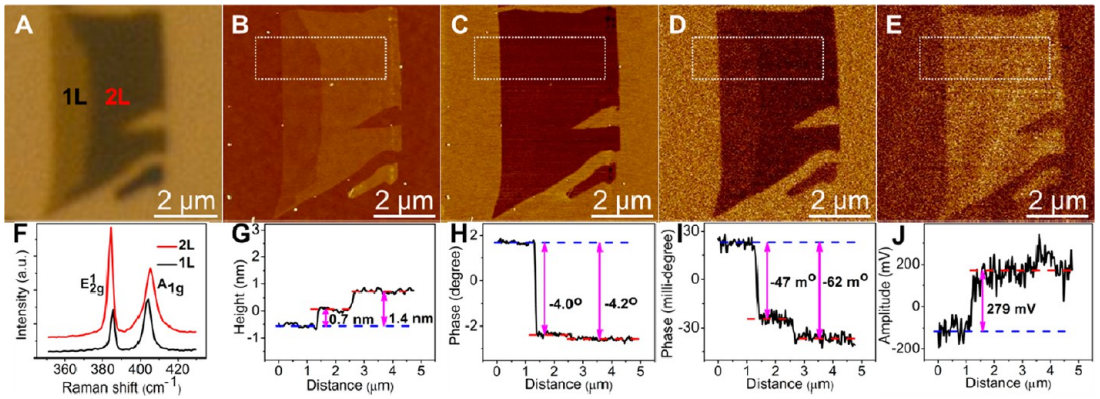

Figure 1. (A) Optical, (B) AFM topography, (C) phase, (D) MFM phase, and (E) MFM amplitude images of 1L and 2L MoS_2 nanosheets on 90 nm SiO_2/Si. (F) Raman spectra of 1L and 2L MoS_2 nanosheets. (G–J) The corresponding profiles of the dashed reactangles in panels B–E. The lift height is 30 nm.

exfoliated, pristine single- and few-layer graphene and MoS_2 nanosheets.

MFM is a powerful tool to detect magnetic interactions between the magnetized AFM tip and nanostructured sample.[39−46] Since MFM can provide nanometer resolution similar to AFM and has ability to detect nanoscopic magnetic domains, it is able to distinguish the magnetic and nonmagnetic responses in the micro- and nanoscale. Therefore, MFM is desirable to characterize the magnetic response of single- or few-layer 2D nanosheets, such as graphene and MoS_2.

Herein, MFM is used to characterize the magnetic responses of mechanically exfoliated single- and few-layer graphene and MoS_2 nanosheets by analysis of the phase and amplitude shifts. Negative phase shift, which represents the attractive interaction between magnetic tip and sample,[40,42,43] was observed in combination with the positive amplitude shift in both single- and few-layer graphene and MoS_2 nanosheets. In addition, we found that the magnetic response of graphene and MoS_2 nanosheets depends on their layer number. However, graphene shows a different thickness-dependent magnetic response compared to MoS_2. Moreover, graphene and MoS_2 flakes become nonmagnetic when they exceed a certain thickness.

RESULTS AND DISCUSSION

In our MFM study, a two-pass tapping/lift mode is used to measure the relatively weak but long-range magnetic interactions in order to minimize the influence of sample topography.[42,45] Each line in the image is scanned twice during the operation of MFM. After a flexible cantilever equipped with a magnetized tip scans over the surface of a sample to obtain the topographic information, the tip is raised up to a certain height (so-called lift height) above the sample surface to measure the magnetic response by monitoring the cantilever's frequency or phase shift in the lift mode scan. Phase shift is used to analyze the magnetic response in the present study due to its higher sensitivity compared to the frequency shift (Figure S1 in Supporting Information).

Figure 1A shows the optical image of a mechanically exfoliated MoS_2 flake on a 90 nm SiO_2-coated Si substrate, referred to as 90 nm SiO_2/Si. AFM and Raman spectroscopy were used to confirm the layer number of the MoS_2 nanosheets. The AFM image in Figure 1B shows that the MoS_2 flake consists of two thickness profiles, that is, 0.7 and 1.4 nm, as measured from its height profile in Figure 1G. It corresponds to the single- (1L) and double-layer (2L) MoS_2 nanosheets,[2,3] which were further confirmed by their in-plane vibration (E^1_{2g}) and out-of-plane vibration (A_{1g}) modes in Raman spectroscopy (Figure 1F).[2,3,47]

MFM was used to characterize the obtained 1L and 2L MoS_2 nanosheets. Figure 1C shows the phase image of the same MoS_2 flake (Figure 1A) obtained simultaneously with the topography image (Figure 1B). Figure 1 panels D and E show the MFM phase and amplitude images of the same flake at a lift height of 30 nm, respectively. Note that in order to avoid the response variation induced by different tips, all images were captured with the same tip. As shown in the AFM phase image (Figure 1C), it is difficult to distinguish the 1L and 2L MoS_2 nanosheets since the difference of phase shift is very small (−4.0° for 1L and −4.2° for 2L, Figure 1H). However, in the MFM phase image, an obvious difference between the 1L and 2L MoS_2 nanosheets is observed (Figure 1D and I). The 2L MoS_2 nanosheet has a bigger negative phase shift than does the 1L MoS_2 (−62 milli-degree (m°) for 2L and −47 m° for 1L), indicating that 2L MoS_2 has stronger attractive interaction with the MFM tip. Meanwhile, Figure 1E shows the MFM amplitude image, in which 1L and 2L MoS_2 nanosheets have positive amplitude shift. In the MFM measurement, the attractive force between tip and sample decreases the resonance frequency of the cantilever,[39,40] resulting in the increase of vibration amplitude signal and decrease of phase signal (Figure S2 in SI). Therefore, the reverse

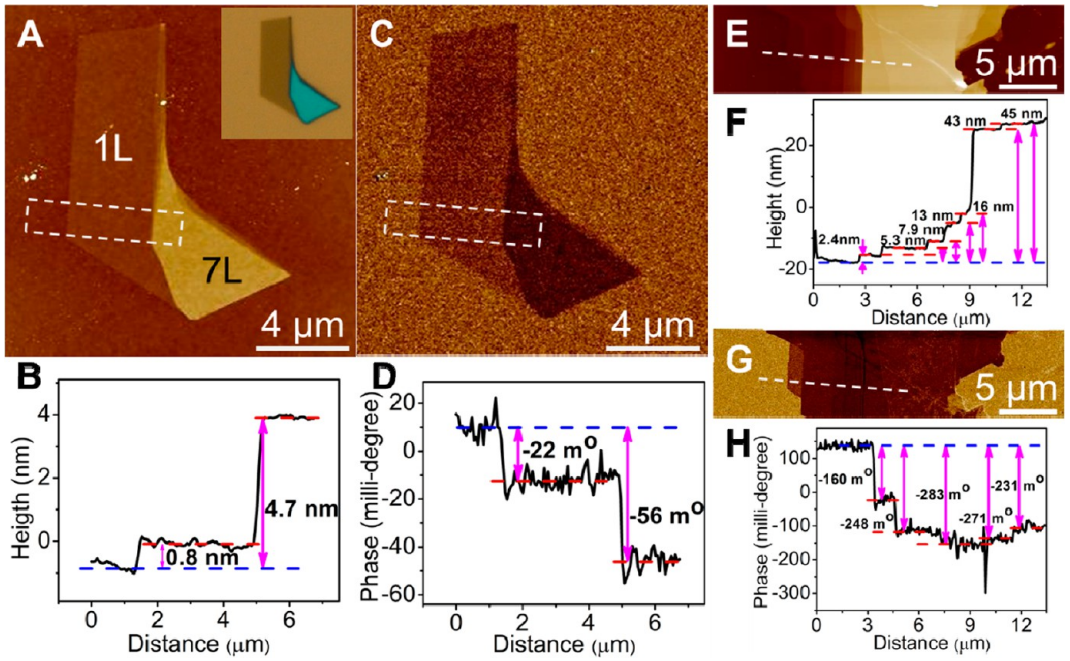

Figure 2. (A) AFM topography and (C) MFM phase images of 1L and 7L MoS_2 nanosheets on 90 nm SiO_2/Si. Inset in panel A is the optical image of a MoS_2 flake. (B, D) The corresponding profiles of the dashed reactangles in panels A and C, respectively. (E) AFM topography and (G) MFM phase images of thick MoS_2 flake. (F, H) The corresponding profiles of the dashed lines in panels E and G, respectively. The lift heights for (C,D) and (G−H) are 30 and 20 nm, respectively.

contrast between MFM phase and amplitude images confirms that 1L and 2L MoS_2 nanosheets are magnetic. Furthermore, our MFM measurement of mechanically exfoliated MoS_2 nanosheets at the decreased lift height gave a larger negative phase shift (Figure S3 in Supporting Information), which also confirmed that the mechanically exfoliated MoS_2 nanosheets are magnetic. It is consistent with the previous reports on the MFM measurement of magnetic samples.[1,42,43,45,46]

As control experiments, the magnetic Fe_3O_4 nanoparticles (NPs) and nonmagnetic gold nanoparticles (Au NPs) were used to confirm the validity of the MFM measurement. As measured by the same MFM tip, magnetic Fe_3O_4 NPs also show negative phase shift in the combination with positive amplitude shift. However, nonmagnetic Au NPs show both positive phase and amplitude shifts (Figure S4 in Supporting Information), which is consistent with previous reports.[41,42,44,45] In this case, the positive phase shift of Au NPs might come from the electrostatic interaction rather than the magnetic interaction.[42] Therefore, aforementioned MFM measurements are valid and able to serve as indication of magnetic response.

Importantly, our experimental results demonstrate that the magnetic response of MoS_2 nanosheets depends on their layer number. As shown in Figure 1D and I, the negative phase shift of the 2L MoS_2 nanosheet increased ~32% (from −47 m° to −62 m°) compared to that of 1L MoS_2. It further increased as the layer number of MoS_2 nanosheets increased to 7L. Figure 2 panels A and C show the AFM topography and MFM phase images of a MoS_2 flake consisting of 1L and 7L MoS_2 nanosheets, respectively, which is confirmed by their thickness (1L, 0.8 nm; 7L, 4.7 nm,[48] Figure 2B). As shown in Figure 2D, the negative phase shift of the 7L MoS_2 nanosheet increases by ~155% (from −22 m° to −56 m°) compared to the 1L MoS_2 nanosheet, indicating the increase of negative phase shift as the layer number increased. Moreover, a further increase of negative phase shift is observed as the thickness of the MoS_2 nanosheet increased from 5.3 nm (8L) to 16 nm (~24L) (Figure 2E−H). There is no noticeable phase shift of MoS_2 nanosheets (from −283 m° to −271 m°) when their thickness increases from 16 nm (~24L) to 43 nm (~66L) (Figure 2E−H). However, the negative phase shift of MoS_2 nanosheets decreases by 18% (from −283 m° to −231 m°) when their thickness increases from 16 nm (~24L) to 45 nm (~69L) (Figure 2E−H). If the thickness further increases to ~183 nm, the MoS_2 flake shows a very weak positive phase shift and positive amplitude shift, implying the thick MoS_2 flake might be nonmagnetic or has no detectable magnetic response (Figure S5 in Supporting Information). This is consistent with a previous report in which it was found that the CVD-grown MoS_2 flakes with a thickness of more than 100 nm showed much weaker magnetism than did the thinner MoS_2 flakes (thickness of ~20 nm).[27]

Moreover, MFM can also be used to characterize the single- and few-layer graphene nanosheets. As shown in Figure 3A, the mechanically exfoliated 1L, 2L, 3L, and 5L graphene nanosheets were successfully deposited

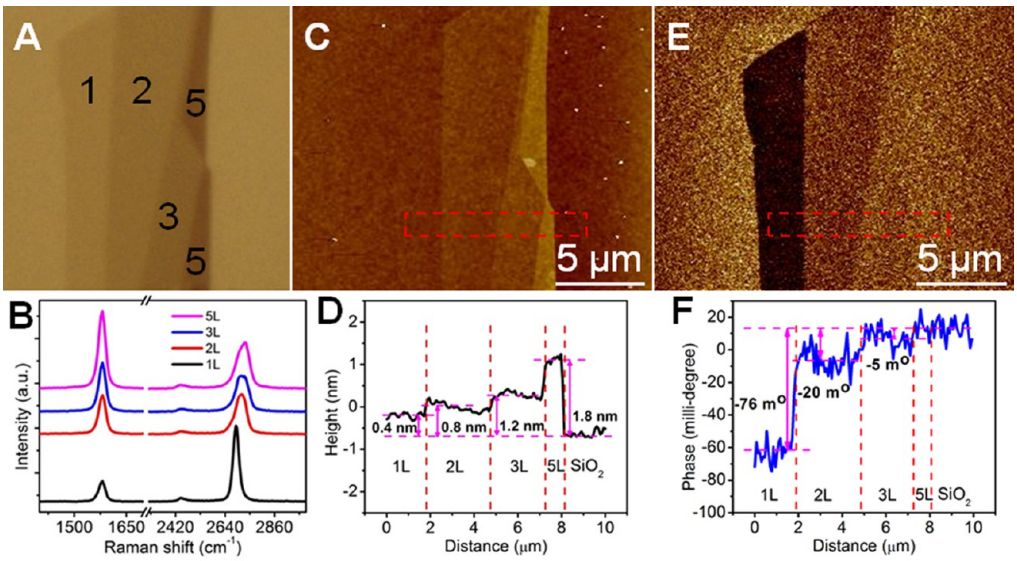

Figure 3. (A) Optical, (C) AFM, and (E) MFM phase images of graphene nanosheets on 90 nm SiO_2/Si. The numbers in panel A indicate the layer number of graphene, which are confirmed by Raman spectroscopy and AFM height profile shown in panels B and D, respectively. (D) AFM height profile and (F) MFM phase shift profile of the dashed rectangles in panels C and E, respectively. The lift height is 30 nm.

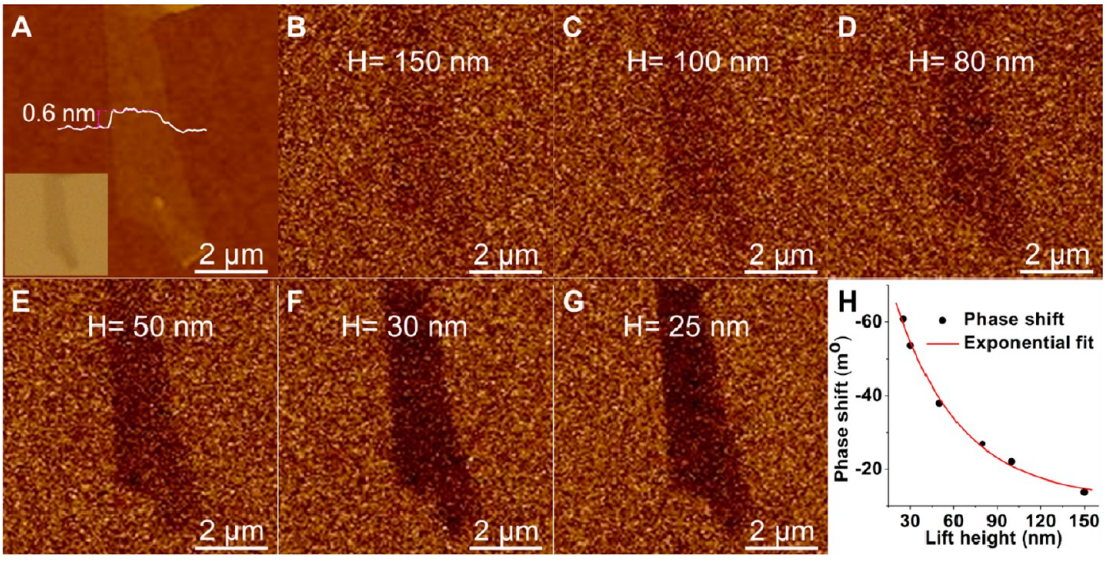

Figure 4. (A) AFM topography and (B–G) MFM phase images of 1L graphene on 90 nm SiO_2/Si at various lift heights: (B) 150, (C) 100, (D) 80, (E) 50, (F) 30, and (G) 25 nm. Inset in panel A: Optical image of the 1L graphene on 90 nm SiO_2/Si. (H) The plot of phase shift *vs* lift height obtained in the MFM measurement on 1L graphene. Red curve is the exponentially fitted curve.

on 90 nm SiO_2/Si, which were confirmed by Raman spectroscopy[49,50] (Figure 3B) and AFM height measurement[51,52] (see Figure 3C and the height profile in Figure 3D), respectively. The corresponding MFM phase image of graphene nanosheets (Figure 3E) shows that 1L graphene has the strongest negative phase shift (~−76 m°), which is larger than that of 2L graphene (~−20 m°) and 3L graphene (~−5 m°) (see the MFM phase shift profile in Figure 3F). However, the 5L graphene nanosheet exhibits almost no phase shift difference from the substrate (see Figure 3E and the MFM phase shift profile in Figure 3F). Furthermore, a thicker graphene flake (*e.g.*, 3 nm thick) showed similar result with the 5L graphene (Figure S6 in Supporting Information). All these results are consistent with a previous study, which reported that the thinner graphene has a larger magnetic signal.[28] Note that graphene nanosheets showed different thickness-dependent magnetic response compared to MoS_2 nanosheets, that is, the negative phase shift of graphene nanosheets decreases as the layer number increases (Figure 3E and F).

It is well-known that the magnetic contrast observed in MFM is highly dependent on the lift height.[39,40,42,46]

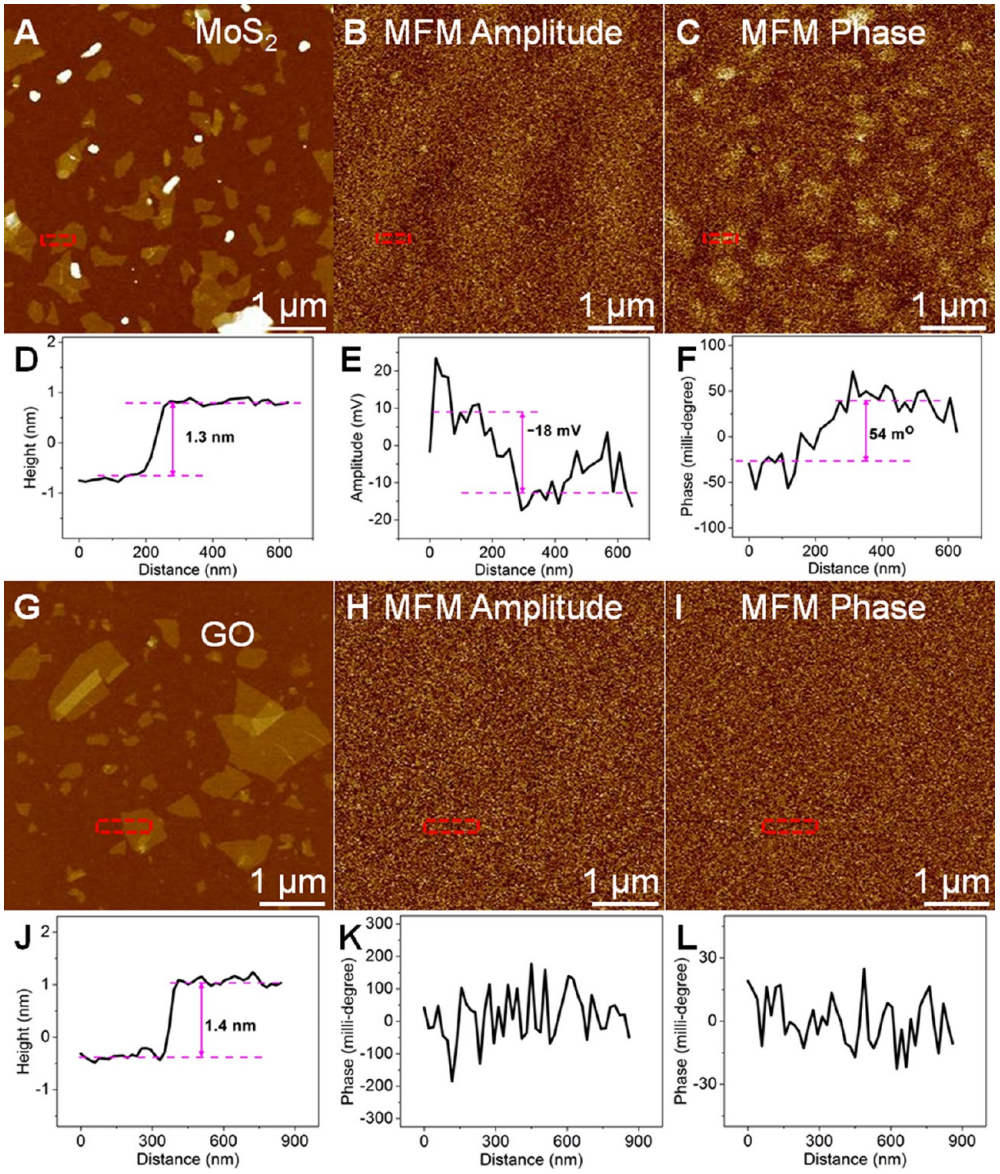

Figure 5. (A, G) AFM topography, (B, H) MFM amplitude and (C, I) MFM phase images of solution-processed single-layer MoS_2 (A, C) and GO (G, I) nanosheets, respectively. (D, J) AFM height, (E, K) MFM amplitude shift and (F, L) MFM phase shift profiles of the dashed red reactangles in (A, C) and (G, I), respectively. Note that the single-layer MoS_2 nanosheet shows negative amplitude shift and positive phase shift, while GO sheets have almost no MFM amplitude and phase shift difference from substrate. The lift height is 30 nm.

To fully characterize the magnetic response of 1L graphene, the MFM phase shift measurement was performed at various lift heights from 25 to 150 nm. Figure 4A shows the AFM image of 1L graphene and the corresponding MFM phase images with lift heights of 150, 100, 80, 50, 30, and 25 nm, respectively (Figure 4B−G). Obviously, the phase shift of 1L graphene is strongly dependent on the lift height. As shown in Figure 4H, the negative phase shift exponentially increases with decreasing the lift height, which is consistent with previous reports.[42,46]

It is worth noting that the aforementioned results are based on the mechanically exfoliated high-quality MoS_2 and graphene nanosheets. The solution-processed 2D nanosheets usually have different properties from those of mechanically exfoliated ones. For example, the mechanically exfoliated 1L MoS_2 nanosheet exhibits n-type behavior,[2,3,8] while the solution-processed one exhibits p-type behavior.[1,22] In this work, MFM was also used to characterize the solution-processed single-layer MoS_2[1] and graphene oxide (GO) nanosheets.[53,54] Figure 5 shows the AFM topography (Figure 5A and G), MFM amplitude (Figure 5B and H) and MFM phase (Figure 5C and I) images of solution-processed MoS_2 and GO nanosheets, respectively. AFM measurement indicates that the heights of MoS_2 and GO nanosheets are 1.3 and 1.4 nm (Figure 5D and J), respectively, confirming that they are single-layer nanosheets, which are consistent with previous reports.[1,54−58] As shown in Figure 5F, the MFM phase measurement of a single-layer MoS_2 nanosheet

shows that the MoS_2 nanosheet has the positive phase shift (~54 m°), indicating that solution-processed single-layer MoS_2 nanosheets might have a repulsive interaction with the MFM tip, which is different from the result of mechanically exfoliated single-layer MoS_2 nanosheets (Figure 1D and Figure 2C). Furthermore, the MFM amplitude measurement shows the weak negative amplitude shift (−18 mV, Figure 5E), which confirms that solution-processed single-layer MoS_2 nanosheets have reverse magnetic signal to the mechanically exfoliated single-layer MoS_2 nanosheets (Figure 1D and E). This difference might arise from the residual lithium on the solution-processed MoS_2 nanosheets, which also exhibited the p-type doping behavior different from the n-type doping behavior of mechanically exfoliated ones.[1−3,22] In addition, the GO nanosheets prepared by the solution method[53,54] have not shown any detectable magnetic response (Figure 5H, I, K, and L), which might be attributed to the presence of functional groups and defects.

CONCLUSION

In summary, for the first time, magnetic force microscopy (MFM) is used to characterize the mechanically exfoliated single- and few-layer MoS_2 and graphene nanosheets. By analysis of phase and amplitude shifts, the magnetic response was found in single- and few-layer MoS_2 and graphene nanosheets. Both MoS_2 and graphene nanosheets showed the thickness-dependent magnetic response. The magnetic response of MoS_2 nanosheets increased as the thickness increased from 0.8 to 16 nm, but decreased as the thickness further increased. However, a too thick MoS_2 flake (>183 nm) has no detectable magnetic response. In contrary to MoS_2 nanosheets, the negative phase shift of graphene nanosheets decreases as the layer number increased. The strongest negative phase shift of graphene nanosheets was found in the single-layer graphene. Even a 5L graphene nanosheet showed almost no detectable phase shift. Compared to the mechanically exfoliated MoS_2 and graphene nanosheets, the solution-processed single-layer MoS_2 nanosheets showed reverse magnetic signal while GO nanosheets exhibited no detectable magnetic response. Our MFM measurement of MoS_2 and graphene nanosheets opens up a useful means for the fundamental understanding of the intrinsic properties of 2D nanomaterials.

METHODS AND MATERIALS

Preparation and MFM Measurements of MoS_2 Nanosheets, Graphene Nanosheets, Fe_3O_4 Nanoparticles (NPs), and Au NPs. Natural graphite (NGS Naturgraphit GmbH, Germany) and MoS_2 crystals (SPI Supplies, USA) were used for the preparation of mechanically exfoliated single- and few-layer graphene and MoS_2 nanosheets, respectively, which were then deposited onto the freshly cleaned 90 nm SiO_2-coated Si substrates (90 nm SiO_2/Si).[2,3] The optical microscope (Eclipse LV100D, Nikon) was used to locate and image the single- and few-layer graphene and MoS_2 nanosheets.

Fe_3O_4 and Au NPs were prepared by using the previously reported method.[55,59] Fe_3O_4 NPs is dispersed in hexane and spin-coated on a 90 nm SiO_2/Si substrate. Au NPs were deposited on a (3-aminopropyl)triethoxysilane-modified 90 nm SiO_2/Si substrate.[55]

Magnetic force microscopy (MFM) was carried out with a commercial AFM instrument (Dimension ICON with NanoScope V controller, Bruker) equipped with a scanner (90 × 90 μm^2) under ambient conditions. Si cantilevers coated with a cobalt/chromium film with the normal resonance frequency of 75 kHz and spring constant of 2.8 N/m (MESP, Bruker) were used for MFM images. The coating produced a coercivity of approximately 400 Oe. Other probes with similar properties (PPP-MFMR, Nanosensors) were also tested and gave similar results. During our MFM measurements, the lift height is 30 nm if there is no specific clarification.

Raman Measurement of MoS_2 and Graphene Nanosheets. Analysis of the single- and few-layer MoS_2 and graphene nanosheets by Raman spectroscopy was carried out on a Renishaw inVia Raman microscope. All spectra were excited at room temperature with laser light (λ = 532 nm) and recorded through the 100× objective. A 2400-lines/mm grating provided a spectral resolution of ~1 cm^{-1}. The Raman spectra were calibrated by using the peak (520 cm^{-1}) of Si substrate.

Conflict of Interest: The authors declare no competing financial interest.

Supporting Information Available: MFM images of thick MoS_2 and graphene flakes, Fe_3O_4 NPs, and Au NPs. MFM phase, amplitude, and frequency images of magnetic recording tape. This material is available free of charge *via* the Internet at http://pubs.acs.org.

Acknowledgment. This work was supported by MOE under AcRF Tier 2 (ARC 10/10, No. MOE2010-T2-1-060), Singapore National Research Foundation under CREATE programme: Nanomaterials for Energy and Water Management, and NTU under Start-Up Grant (M4080865.070.706022) in Singapore.

REFERENCES AND NOTES

1. Zeng, Z. Y.; Yin, Z. Y.; Huang, X.; Li, H.; He, Q. Y.; Lu, G.; Boey, F.; Zhang, H. Single-Layer Semiconducting Nanosheets: High-Yield Preparation and Device Fabrication. *Angew. Chem., Int. Ed.* **2011**, *50*, 11093–11097.
2. Li, H.; Lu, G.; Yin, Z. Y.; He, Q. Y.; Li, H.; Zhang, Q.; Zhang, H. Optical Identification of Single- and Few-Layer MoS_2 Sheets. *Small* **2012**, *8*, 682–686.
3. Li, H.; Yin, Z. Y.; He, Q. Y.; Li, H.; Huang, X.; Lu, G.; Fam, D. W. H.; Tok, A. I. Y.; Zhang, Q.; Zhang, H. Fabrication of Single- and Multilayer MoS_2 Film-Based Field-Effect Transistors for Sensing NO at Room Temperature. *Small* **2012**, *8*, 63–67.
4. Novoselov, K. S.; Geim, A. K.; Morozov, S. V.; Jiang, D.; Zhang, Y.; Dubonos, S. V.; Grigorieva, I. V.; Firsov, A. A. Electric Field Effect in Atomically Thin Carbon Films. *Science* **2004**, *306*, 666–669.
5. Novoselov, K. S.; Jiang, D.; Schedin, F.; Booth, T. J.; Khotkevich, V. V.; Morozov, S. V.; Geim, A. K. Two-Dimensional Atomic Crystals. *Proc. Natl. Acad. Sci. U.S.A.* **2005**, *102*, 10451–10453.
6. Coleman, J. N.; Lotya, M.; O'Neill, A.; Bergin, S. D.; King, P. J.; Khan, U.; Young, K.; Gaucher, A.; De, S.; Smith, R. J.; *et al.* Two-Dimensional Nanosheets Produced by Liquid Exfoliation of Layered Materials. *Science* **2011**, *331*, 568–571.
7. Huang, X.; Yin, Z. Y.; Wu, S. X.; Qi, X. Y.; He, Q. Y.; Zhang, Q. C.; Yan, Q. Y.; Boey, F.; Zhang, H. Graphene-Based Materials:

Synthesis, Characterization, Properties, and Applications. *Small* **2011**, *7*, 1876–1902.
8. Radisavljevic, B.; Radenovic, A.; Brivio, J.; Giacometti, V.; Kis, A. Single-Layer MoS_2 Transistors. *Nat. Nanotechnol.* **2011**, *6*, 147–150.
9. Huang, X.; Qi, X.; Boey, F.; Zhang, H. Graphene-Based Composites. *Chem. Soc. Rev.* **2012**, 666–686.
10. Huang, X.; Zeng, Z.; Fan, Z.; Liu, J.; Zhang, H. Graphene-Based Electrodes. *Adv. Mater.* **2012**, *24*, 5979–6004.
11. He, Q. Y.; Wu, S. X.; Yin, Z. Y.; Zhang, H. Graphene-Based Electronic Sensors. *Chem. Sci.* **2012**, *3*, 1764–1772.
12. Li, H.; Lu, G.; Wang, Y.; Yin, Z.; Cong, C.; He, Q.; Wang, L.; Ding, F.; Yu, T.; Zhang, H. Mechanical Exfoliation and Characterization of Single- and Few-Layer Nanosheets of WSe_2, TaS_2, and $TaSe_2$. *Small* **2013**, 10.1002/smll.201202919.
13. Castellanos-Gomez, A.; Agrait, N.; Rubio-Bollinger, G. Optical Identification of Atomically Thin Dichalcogenide Crystals. *Appl. Phys. Lett.* **2010**, *96*, 213116.
14. Lee, C.; Li, Q. Y.; Kalb, W.; Liu, X. Z.; Berger, H.; Carpick, R. W.; Hone, J. Frictional Characteristics of Atomically Thin Sheets. *Science* **2010**, *328*, 76–80.
15. Mak, K. F.; Lee, C.; Hone, J.; Shan, J.; Heinz, T. F. Atomically Thin MoS_2: A New Direct-Gap Semiconductor. *Phys. Rev. Lett.* **2010**, *105*, 136805.
16. Benameur, M. M.; Radisavljevic, B.; Heron, J. S.; Sahoo, S.; Berger, H.; Kis, A. Visibility of Dichalcogenide Nanolayers. *Nanotechnology* **2011**, *22*, 125706.
17. Yin, Z. Y.; Li, H.; Li, H.; Jiang, L.; Shi, Y. M.; Sun, Y. H.; Lu, G.; Zhang, Q.; Chen, X. D.; Zhang, H. Single-Layer MoS_2 Phototransistors. *ACS Nano* **2012**, *6*, 74–80.
18. Huang, X.; Zeng, Z. Y.; Zhang, H. Metal Dichalcogenide Nanosheets: Preparation, Properties and Applications. *Chem. Soc. Rev.* **2013**, 1934–1946.
19. Chhowalla, M.; Shin, H. S.; Eda, G.; Li, L. J.; Loh, K.; Zhang, H. The Chemistry of Ultra-thin Transition Metal Dichalcogenide Nanosheets. *Nat. Chem.* **2013**, 10.1038/nchem.1589.
20. Liu, H.; Neal, A. T.; Ye, P. D. Channel Length Scaling of MoS_2 MOSFETs. *ACS Nano* **2012**, *6*, 8563–8569.
21. Wu, S.; Zeng, Z.; He, Q.; Wang, Z.; Wang, S. J.; Du, Y.; Yin, Z.; Sun, X.; Chen, W.; Zhang, H. Electrochemically Reduced Single-Layer MoS_2 Nanosheets: Characterization, Properties, and Sensing Applications. *Small* **2012**, *8*, 2264–2270.
22. He, Q.; Zeng, Z.; Yin, Z.; Li, H.; Wu, S.; Huang, X.; Zhang, H. Fabrication of Flexible MoS_2 Thin-Film Transistor Arrays for Practical Gas-Sensing Applications. *Small* **2012**, *8*, 2994–2999.
23. Liu, J.; Zeng, Z.; Cao, X.; Lu, G.; Wang, L.-H.; Fan, Q.-L.; Huang, W.; Zhang, H. Preparation of MoS_2–Polyvinylpyrrolidone Nanocomposites for Flexible Nonvolatile Rewritable Memory Devices with Reduced Graphene Oxide Electrodes. *Small* **2012**, *8*, 3517–3522.
24. Yin, Z.; Zeng, Z.; Liu, J.; He, Q.; Chen, P.; Zhang, H. Memory Devices Using a Mixture of MoS_2 and Graphene Oxide as the Active Layer. *Small* **2013**, 10.1002/smll.201201940.
25. Zhou, W.; Yin, Z.; Du, Y.; Huang, X.; Zeng, Z.; Fan, Z.; Liu, H.; Wang, J.; Zhang, H. Synthesis of Few-Layer MoS_2 Nanosheet-Coated TiO_2 Nanobelt Heterostructures for Enhanced Photocatalytic Activities. *Small* **2013**, *9*, 140–147.
26. Chang, Y.-H.; Lin, C.-T.; Chen, T.-Y.; Hsu, C.-L.; Lee, Y.-H.; Zhang, W.; Wei, K.-H.; Li, L.-J. Highly Efficient Electrocatalytic Hydrogen Production by MoS_x Grown on Graphene-Protected 3D Ni Foams. *Adv. Mater.* **2013**, *25*, 756–760.
27. Zhang, J.; Soon, J. M.; Loh, K. P.; Yin, J. H.; Ding, J.; Sullivian, M. B.; Wu, P. Magnetic Molybdenum Disulfide Nanosheet Films. *Nano Lett.* **2007**, *7*, 2370–2376.
28. Matte, H. S. S. R.; Subrahmanyam, K. S.; Rao, C. N. R. Novel Magnetic Properties of Graphene: Presence of Both Ferromagnetic and Antiferromagnetic Features and Other Aspects. *J. Phys. Chem. C* **2009**, *113*, 9982–9985.
29. Wang, Y.; Huang, Y.; Song, Y.; Zhang, X. Y.; Ma, Y. F.; Liang, J. J.; Chen, Y. S. Room-Temperature Ferromagnetism of Graphene. *Nano Lett.* **2009**, *9*, 220–224.
30. Mathew, S.; Gopinadhan, K.; Chan, T. K.; Yu, X. J.; Zhan, D.; Cao, L.; Rusydi, A.; Breese, M. B. H.; Dhar, S.; Shen, Z. X.; *et al.* Magnetism in MoS_2 Induced by Proton Irradiation. *Appl. Phys. Lett.* **2012**, *101*, 102103.
31. Tongay, S.; Varnoosfaderani, S. S.; Appleton, B. R.; Wu, J. Q.; Hebard, A. F. Magnetic Properties of MoS_2: Existence of Ferromagnetism. *Appl. Phys. Lett.* **2012**, *101*, 123105.
32. Rao, C. N. R.; Matte, H. S. S. R.; Subrahmanyam, K. S.; Maitra, U. Unusual Magnetic Properties of Graphene and Related Materials. *Chem. Sci.* **2012**, *3*, 45–52.
33. Botello-Mendez, A. R.; Lopez-Urias, F.; Terrones, M.; Terrones, H. Metallic and Ferromagnetic Edges in Molybdenum Disulfide Nanoribbons. *Nanotechnology* **2009**, *20*, 325703.
34. Shidpour, R.; Manteghian, M. A Density Functional Study of Strong Local Magnetism Creation on MoS_2 Nanoribbon by Sulfur Vacancy. *Nanoscale* **2010**, *2*, 1429–1435.
35. Esquinazi, P.; Spemann, D.; Hohne, R.; Setzer, A.; Han, K. H.; Butz, T. Induced Magnetic Ordering by Proton Irradiation in Graphite. *Phys. Rev. Lett.* **2003**, *91*, 227201.
36. Mcclure, J. W. Diamagnetism of Graphite. *Phys. Rev.* **1956**, *104*, 666–671.
37. Hong, J. M.; Bekyarova, E.; Liang, P.; de Heer, W. A.; Haddon, R. C.; Khizroev, S. Room-Temperature Magnetic Ordering in Functionalized Graphene. *Sci. Rep.* **2012**, *2*, 624.
38. Hong, J. M.; Niyogi, S.; Bekyarova, E.; Itkis, M. E.; Ramesh, P.; Amos, N.; Litvinov, D.; Berger, C.; de Heer, W. A.; Khizroev, S.; *et al.* Effect of Nitrophenyl Functionalization on the Magnetic Properties of Epitaxial Graphene. *Small* **2011**, *7*, 1175–1180.
39. Hartmann, U. Magnetic Force Microscopy. *Annu. Rev. Mater. Sci.* **1999**, *29*, 53–87.
40. Rugar, D.; Mamin, H. J.; Guethner, P.; Lambert, S. E.; Stern, J. E.; Mcfadyen, I.; Yogi, T. Magnetic Force Microscopy: General-Principles and Application to Longitudinal Recording Media. *J. Appl. Phys.* **1990**, *68*, 1169–1183.
41. Zhang, Y.; Yang, M.; Ozkan, M.; Ozkan, C. S. Magnetic Force Microscopy of Iron Oxide Nanoparticles and Their Cellular Uptake. *Biotechnol. Prog.* **2009**, *25*, 923–928.
42. Neves, C. S.; Quaresma, P.; Baptista, P. V.; Carvalho, P. A.; Araujo, J. P.; Pereira, E.; Eaton, P. New Insights into the Use of Magnetic Force Microscopy to Discriminate between Magnetic and Nonmagnetic Nanoparticles. *Nanotechnology* **2010**, *21*, 305706.
43. Mohamed, H. D. A.; Watson, S. M. D.; Horrocks, B. R.; Houlton, A. Magnetic and Conductive Magnetite Nanowires by DNA-Templating. *Nanoscale* **2012**, *4*, 5936–5945.
44. Sievers, S.; Braun, K. F.; Eberbeck, D.; Gustafsson, S.; Olsson, E.; Schumacher, H. W.; Siegner, U. Quantitative Measurement of the Magnetic Moment of Individual Magnetic Nanoparticles by Magnetic Force Microscopy. *Small* **2012**, *8*, 2675–2679.
45. Kim, D.; Chung, N. K.; Allen, S.; Tendler, S. J. B.; Park, J. W. Ferritin-Based New Magnetic Force Microscopic Probe Detecting 10 nm Sized Magnetic Nanoparticles. *ACS Nano* **2012**, *6*, 241–248.
46. Hsieh, C. W.; Zheng, B.; Hsieh, S. Ferritin Protein Imaging and Detection by Magnetic Force Microscopy. *Chem. Commun.* **2010**, *46*, 1655–1657.
47. Lee, C.; Yan, H.; Brus, L. E.; Heinz, T. F.; Hone, J.; Ryu, S. Anomalous Lattice Vibrations of Single- and Few-Layer MoS_2. *ACS Nano* **2010**, *4*, 2695–2700.
48. Since the theoretical thickness of 1L MoS_2 is 0.65 nm, 4.7 nm of MoS_2 represents 7L.
49. Ferrari, A. C.; Meyer, J. C.; Scardaci, V.; Casiraghi, C.; Lazzeri, M.; Mauri, F.; Piscanec, S.; Jiang, D.; Novoselov, K. S.; Roth, S.; *et al.* Raman Spectrum of Graphene and Graphene Layers. *Phys. Rev. Lett.* **2006**, *97*, 187401.
50. Yoon, D.; Moon, H.; Cheong, H.; Choi, J. S.; Choi, J. A.; Park, B. H. Variations in the Raman Spectrum as a Function of the Number of Graphene Layers. *J. Korean Phys. Soc.* **2009**, *55*, 1299–1303.
51. Xu, K.; Cao, P. G.; Heath, J. R. Graphene Visualizes the First Water Adlayers on Mica at Ambient Conditions. *Science* **2010**, *329*, 1188–1191.
52. Ishigami, M.; Chen, J. H.; Cullen, W. G.; Fuhrer, M. S.; Williams, E. D. Atomic Structure of Graphene on SiO_2. *Nano Lett.* **2007**, *7*, 1643–1648.

53. Li, H.; Cao, X.; Li, B.; Zhou, X.; Lu, G.; Liusman, C.; He, Q.; Boey, F.; Venkatraman, S. S.; Zhang, H. Single-Layer Graphene Oxide Sheet: A Novel Substrate for Dip-Pen Nanolithography. *Chem. Commun.* **2011**, *47*, 10070–10072.
54. Zhou, X.; Huang, X.; Qi, X.; Wu, S.; Xue, C.; Boey, F. Y. C.; Yan, Q.; Chen, P.; Zhang, H. *In Situ* Synthesis of Metal Nanoparticles on Single-Layer Graphene Oxide and Reduced Graphene Oxide Surfaces. *J. Phys. Chem. C* **2009**, *113*, 10842–10846.
55. Li, H.; Zhang, J.; Zhou, X. Z.; Lu, G.; Yin, Z. Y.; Li, G. P.; Wu, T.; Boey, F.; Venkatraman, S. S.; Zhang, H. Aminosilane Micropatterns on Hydroxyl-Terminated Substrates: Fabrication and Applications. *Langmuir* **2010**, *26*, 5603–5609.
56. Schumacher, A.; Scandella, L.; Kruse, N.; Prins, R. Single-Layer Mos_2 on Mica: Studies by Means of Scanning Force Microscopy. *Surf. Sci.* **1993**, *289*, L595–L598.
57. Eda, G.; Yamaguchi, H.; Voiry, D.; Fujita, T.; Chen, M. W.; Chhowalla, M. Photoluminescence from Chemically Exfoliated MoS_2. *Nano Lett.* **2011**, *11*, 5111–5116.
58. Qi, X. Y.; Pu, K. Y.; Li, H.; Zhou, X. Z.; Wu, S. X.; Fan, Q. L.; Liu, B.; Boey, F.; Huang, W.; Zhang, H. Amphiphilic Graphene Composites. *Angew. Chem., Int. Ed.* **2010**, *49*, 9426–9429.
59. Park, J.; An, K. J.; Hwang, Y. S.; Park, J. G.; Noh, H. J.; Kim, J. Y.; Park, J. H.; Hwang, N. M.; Hyeon, T. Ultra-Large-Scale Syntheses of Monodisperse Nanocrystals. *Nat. Mater.* **2004**, *3*, 891–895.